Estimation of Mass Flow of Seeds using Fibre Sensor and Multiple Linear Regression Modelling

A. A. Al-Mallahi[1], T. Kataoka[2]

[1] Post-Doctoral Fellow, Graduate School of Agriculture, Hokkaido University, Kita-9, Nishi-9, Kita-ku, Sapporo Hokkaido 060-8589, Japan, Email: ahmad@bpe.agr.hokudai.ac.jp, Tel: +81117063831, Fax: +817062555

[2] Research Faculty of Agriculture, Hokkaido University, Kita-9, Nishi-9, Kita-ku, Sapporo Hokkaido 060-8589, Japan

Abstract

A new methodology to estimate the mass of grain seeds, which flow in the shape of clumps, was suggested in this paper. The methodology used an off-the-shelf digital fibre sensor to detect the behaviour of the clumps and multiple linear regression modelling to estimate the mass by the parameters detected by the sensor which were the length and the density of the clumps.

An indoor apparatus was used for modelling which resembled the sowing process using the grain drill. A fluted roller was installed in the apparatus to regulate the flow of seeds. It was rotated by a motor at 2, 4 and 6 rpm to cover all the possible mass flow rates which might occur during actual sowing. Modelling was based on several assumptions, such as the linearity between the sensor parameters and the mass. Although errors were observed while estimating each clump independently, the methodology was able to estimate the mass of a continuous flow of seed clumps. The average difference in estimation at 4 rpm was 0.9%, while there was overestimation at 2 rpm and underestimation at 6 rpm resulting in an overall estimation error of 5.3%. These results showed that the digital fibre sensor could be used for estimating mass flow of seeds at variable sowing rates within the speed limits of the grain drill.

Keywords: Mass flow, Sowing, Regression analysis, Fibre sensor

Nomenclature			
n	Natural number $\{1, 2, 3, \ldots\}$	a	Initial value of voltage output
t	Period of time	d	Density of clump during one period of time
l	Length of clump during one period of time	m	Mass of clumps during one period of time
v	Value of voltage output during the experiment	$ß_i$	Coefficient of the i-th variable

1. Introduction

Achieving seed sowing uniformity during planting might be the most important factor in maximizing the yield of the crop. In grain drills, sowing is regulated using fluted rollers which drop seeds toward pipes in clumps containing more than one seed at a time. The rotation of the fluted rollers is caused by the rotation of the tyres of the grain drill itself. Although the variation in the flow of seeds cannot be completely avoided due to the nature of the fluted rollers, it is common to calibrate the grain drill prior sowing, so as to optimise the uniformity of sowing per unit area. However, the actual distribution of seeds in a farm cannot be grasped because there is no feedback mechanism about the flow of seeds during sowing. Moreover, the propelling tractor may run during seeding at speeds ranging between 5-9 km/h, which means that the

sowing rate per time varies considerably by two factors namely, the formation of clumps due to the fluted roller and the changes in tractor speed.

In order to estimate the seed distribution by a 1 certain fluted roller, laboratory tests are performed so that the patterns, in which seeds flow at different rates, are obtained. This procedure helps in estimating the seed flow in practice while the grain drill is propelled by the tractor in the farm at different speeds. Traditionally, these laboratory tests aim to investigate the spacing between seeds which have relatively large diameters such as sugar beets. The tests are conducted using a sticky conveyor belt running at a certain speed underneath the pipe in which seeds are flowing. The sticky belt receives the falling seeds which lay on the belt without bouncing. The flow of the seeds can be calculated by counting the number of seeds passing a certain point on the conveyor belt per unit time. In order to avoid human error in counting seeds especially at high rates, different computerized systems were developed recently (Onal, 2009; Navid, 2011).

However, since there are many limitations in conducting tests using sticky belts, different approaches were developed recently. Kocher et al (1998) and Lan et al (1999) used opto-electronic sensor system to measure sugar beet seed spacing. On the other hand, Karayel et al (2006) used a high speed camera system to measure the spacing for wheat seeds which flow in much higher rates than sugar beets.

In order to estimate high rate flows in real time, Grift (2001) developed a model for mass flow measurement of granular materials and tested it using simulation. Next, Grift et al (2001) validated the model by laboratory experiments. The objective of these

researches was to estimate the flow rate of granular fertilizer materials in aerial application which flow in a pattern similar to the wheat seeds in the pipes of the grain drill; that is, in clumps containing multiple particles with varying diameters. 1 The sensor, used in these researches, is described in Grift and Hofstee (1997). It is an array of optical sensors which are connected in one OR function so that the sensor would detect the passage of a clump if at least one of the optical sensors was blocked. Lately, Grift and Crespi (2008a; 2008b) estimated the flow rate of free falling granular particles and their diameters using the same sensor. They used converging and diverging lenses to assure the detection of each falling particle in the tube.

In this research, the objective was to develop a methodology to estimate the mass of grain seeds during sowing, which flow in rates higher than sugar beets but lower than fertilizers. Therefore, a laboratory apparatus, able to regulate the flow of seeds, was firstly built. Then, an off-the-shelf light sensor was installed to detect the flow of seeds. Finally, a statistical model to estimate the mass of flowing seeds was developed and validated based on data obtained from the sensor.

2. Materials and Methods

2.1. Seeds

Rye seeds of an average of 33 seeds per gram were used in this study. The seeds have elongated shape with an approximate average width of 2 mm while the average length is 7 mm. In Hokkaido, the average sowing rate of rye is 100 kg/ha, which is the same rate of applying other grain seeds such as wheat.

2.2. Digital Fibre sensor

The sensor used to detect the flow of seeds was an 1 off-the-shelf digital fibre sensor (Keyence, FS-N10). It consists of a light transmitter and receiver as well as an amplifier connected by fibre cables as shown in the sketch of Figure 1. The amplifier functions as a light source, sent toward the emitter using one fibre cable, and receive the light from the receiver using another cable. Light of wavelength 620 nm travels from the emitter toward the receiver in the shape of a beam of 40 × 3 mm over the pipe where seeds will fall into, covering its whole diameter. When the beam of light is interrupted by seeds, their shade will fall on the surface of the receiver causing difference in intensity. The amplifier translates the intensity difference into a signal of voltage output.

2.3. Indoor apparatus

In order to examine the ability of the fibre sensor to detect mass flow of seeds, an indoor apparatus was built. Figure 2 shows a sketch of the apparatus which consisted of a hopper, a fluted roller to regulate the mass flow, an electrical motor, a digital scale, the digital fibre sensor, and platforms for the roller and the sensor. A laptop was used to collect data from the fibre sensor and the digital scale simultaneously.

Seeds filled in the hopper flow through pipes toward the fluted roller (Tume, KL 2500J, PN-96560001) which is rated so that it delivers 0.8 g/m when the grain drill is set at 100kg/ha. The AC electrical motor (Mitsubishi, HC-MFS23B) was connected to the laptop through a servo amplifier (Mitsubishi, MR-J2S-10A) so as to control the rotational speed of its shaft. In order to resemble the operation of the grain drill at 7 km/h, the electrical motor was set to run at 4 rpm. Next, the rotational speed was set at 2

and 6 rpm to cover the whole range of possible forward speeds of the tractor. The seeds falling from the feeding roller passed through a hole in the platform on which the emitter and the receiver of the fibre sensor were installed on both sides. Data about the intensity of light received from the sensor were transferred to the laptop using a card bus (Interface, CSI-320312). The seeds finally fell in a container placed on the digital scale (A&D, GF300) which was connected to the laptop.

2.4. Data collection

The experiment was consisted of several trials of running the motor on a constant rotational speed. Table 1 shows the speed of motor, the total time interval of each trial and the total actual mass flowed during the trial, as well as the estimated mass calculated and the percentage of error of estimation. The target was to collect more or less the same mass of seeds at different total time intervals so as to obtain a variable mass flow similar to that generated by a grain drill in the farm.

While seeds were interrupting the light beam onto the scale in each trial, the sensor output data as well as the accumulative mass of seeds were sampled and registered simultaneously in the laptop. However, the frequency of data sampling by both devices was different as it was 1.25 Hz and 10 Hz for the scale and the sensor respectively. To overcome the mismatching in the frequency, a simple calculation was made first. The shortest time interval in which mass data could be sampled by the scale was 0.8 s.

Dividing the frequency of the sensor data sampling on the frequency of the scale data sampling, the number of times data were sampled by the sensor was 8 times the number of data sampled by the scale. This difference in sampling 1 was considered while

building up the modelling equations described henceforth.

Because a fluted wheel was used to regulate the mass flow of seeds, the flow took the shape of clumps of variable number of seeds. An example of the variation in the mass of the clumps is shown in Figure 3, where the mass of the clumps is plotted against time in the shape of spikes which appeared whenever a new clump hit the scale. Although the length of each clump could not be estimated separately, the number of times the beam of light was interrupted, within a certain period of time (*t*), was assumed as the length of the clump (*l*).

Also, the variation in the light intensity was assumed as the bulk density of the clumps (*d*) within the same period of time (*t*) which was calculated using,

$$t = 0.8n \tag{1}$$

where the value (0.8) represents the shortest time interval in which the mass could be measured by the scale. The length (*l*) could be calculated using,

$$l = \sum_{k=1}^{8n} b_k \tag{2}$$

while,

$$b = \begin{cases} 1, & v < a \\ 0, & v \geq a \end{cases} \tag{3}$$

where the value (8) represents the number of times data are sampled by the sensor amplifier during the shortest time interval. Equations (2) and (3) indicate that the length was represented by counting the number of times the beam 1 of light was interrupted in a certain period of time. Finally, the density was calculated using,

$$d = 8an - \sum_{k=1}^{8n} v_k \quad (4)$$

where the initial output value (a) of the sensor in Equations (3) and (4) was set to 4.91 volts throughout the experiment, and the value (8) represents the number of times data are sampled by the sensor amplifier during the shortest time interval. Equation 4 indicates that the bulk density was represented by the drop of light intensity during a certain period of time. Thus, the mass of seeds (m) within a certain period of time was considered as a function of the length and bulk density of all clumps as summarized in Equation 5:

$$m = f(d, l) \quad (5)$$

Figure 4 shows a practical example of how the raw data sampled from the fibre sensor and the scale were arranged in sets of variables according to the desired period of time. The left table of the figure shows the raw data as they are sampled and registered in the laptop during 3.2 s. Since the sampling frequency was 10 Hz and 1.25 Hz for the fibre sensor and the scale, the number of collected data was 32 and 4 respectively. The right table of the figure shows how the sampled data were arranged in sets of variables which consisted of the clump length (l) and bulk density (d) versus the mass of 1 the clump (m). Three periods of time at n = 1, 2, and 3 i.e., at 0.8, 1.6, and 2.4 s respectively, were chosen to study the effect of changing the period of time on the accuracy of estimation. At n = 1, three sets of variables were calculated, while at n = 2 and n = 3, one set of variables was collected at each period. These 5 sets of variables are shown in grey in the right table of the figure. The sets of variables which are listed above and under the ones in grey were calculated from the raw data beyond the 3.2 s shown in the figure.

Table 2 shows the total number of clumps obtained after arranging the raw data in each trial. Although 6 trials were performed initially at each speed, the total number of trials was, as 3 trials at the speed of 2 rpm were disregarded due to data corruption. Nevertheless, the number of clumps was considered adequate since the time at 2 rpm was longer. Clumps of Trials 1, 4, 7, 10 and 13 (Table 1) were used for modelling while clumps obtained from the other trials were used for validation. Eventually, the number of clumps used for modelling was 405, 275, and 150 for the estimation models at the periods of time of 0.8, 1.6, and 2.4 s respectively, which was, roughly, one-fourth of the total number of clumps.

2.5. Linear regression modelling

Assuming linear relationships between the parameters at a specific range of masses and assuming that the parameters are independent, Equation 5 could be written as

$$m = ß_0 + ß_1 d + ß_2 l \quad (6)$$

which is the general formula of an empirical multiple 1 linear regression equation. The final assumption was that the mass should be zero when the values of both density and width are zero. Hence, the coefficient *ß0* could be eliminated and the equation was eventually rewritten as;

$$m = ß_1 d + ß_2 l \quad (7)$$

The coefficients *ß1* and *ß2* were calculated using the "*lm* function" of the R environment (R-Project, 2007) in which the modelling data described earlier were applied. One model was prepared for each period of time and the values of the coefficients are shown

in Table 3.

3. Results and discussion

3.1. Mass estimation using models of different periods of time

Table 3 indicates that the values of the coefficients of the different models were very similar. This observation could be enhanced when the models were used to estimate the overall mass. For instance, at Trial 4 the overall estimated mass of the flow using the three models were identical and equalled 230.3 gram, whereas the overall actual mass was 236.8 gram as mentioned in Table 1. Moreover, it was found that the actual masses of the clumps, measured by the scale, and the estimated masses, calculated by the models, were resembled in the same pattern regardless the period of time. Figure 5 illustrates the actual variation in the clumps, measured using the scale, versus the estimated clumps, using the estimation model, at Trial 4 whose data were one of the data sets used to create the estimation model.

The trial lasted for 110 s but was interrupted for 1 approximately 25 s by stopping the rotating motor, which made the total interval longer than other trials at 4 rpm as described in Table 1. Since the model was based on assuming that clumps were falling in fixed periods of time, it was anticipated that the models of longer periods of time would be more accurate in estimating the mass of each clump. However, Figure 5 (a) shows that the curve of the estimated masses was following the curve of the actual masses at each spike, indicating that all the clumps were detected by the sensor. Nevertheless, the spikes of the actual masses seemed sharper than the spikes of the estimated masses occasionally. This may have occurred because of the overlap of one

clump between two periods of time which have resulted in an underestimated mass followed by an overestimated one or vice versa. Fixing the period of time may have affected the instantaneous estimation of some of the clumps.

However, this observation was the same even when the period of time was extended. Therefore, evaluating the ability of the model to estimate mass at different speeds was performed at the shortest period of time.

3.2. Mass estimation of variable flow

3.2.1. Variation of clump size at constant rotational speed of the fluted roller

The total number of clumps at 0.8 s was 1903. In order to study the effect of the size of the clumps on the estimation, an arbitrary threshold was made so that clumps whose masses exceeded one gram were considered as heavy clumps, while lighter clumps were considered as light. Figure 6 shows the relationship between the actual and estimated masses of all clumps, whether heavy or light, collected 1 during the 15 trials when the period of time was 0.8 s. The figure shows that the model overestimated most of the light clumps, while a more moderate distribution around the straight line was observed otherwise.

However, a tendency to underestimate the clumps was also observed at heavier clumps. Heavy clumps consisted of a big number of seeds passing instantaneously in front of the sensor. Since the sensor was able to detect the seeds from one side only, some seeds were occluded, causing the underestimation. Despite the inaccuracy in estimating the mass of each clump separately, the model had high accuracy in estimating the mass

flow which consisted of successive clumps of different sizes because they were falling in a similar pattern throughout the trial. In other words, the model was able to detect the pattern in which clumps interrupt the light beam and translate this pattern into mass estimation. Figure 7 illustrates the relationship in estimating the mass flow of each trial entirely. The model had the best estimating results when the roller speed was 4 rpm, as the average error was 0.9%. At 2 rpm, there was an overestimation, which ranged approximately between 4% and 10%. On the other hand, there was an underestimation at 6 pm, which ranged approximately between 5% and 12%. The overall estimation error of the whole experiment was 5.3% calculated by averaging the absolute values of error of the 15 trials illustrated in the bottom of Table 1.

3.2.2. Effects of Varying the rotational speed on mass estimation

The results discussed in 3.2.1 suggest that the variation in the rotational speed might be a limiting factor on the ability of the model to estimate mass at a wide range of speeds. Table 4 shows the average number of heavy clumps 1 at the different speeds of the roller, their percentage as mass of the overall mass, the frequency in which they occur, as well as their average and maximum masses. The table indicates that changing the speed had more effects on the frequency of the heavy clumps more than on their sizes. For instance, the average frequency at 6 rpm was 2.8 times higher than the mass at 2 rpm, whereas the average mass at 6 rpm was 1.3 times higher than that at 2 rpm.

On one hand, the assumption that the length of a clump is equal to the number of times the light beam is interrupted indicates that the length parameter ($ß_1$) would be affected by the speed in which the seeds fall. On the other hand, the assumption that the density

of the clump is equal to the differences in light intensity of the sensor indicates that the density parameter ($ß_2$) would be affected by the pattern in which clumps are formed. While the former ($ß_1$) would depend solely on the rotational speed of the roller, the latter ($ß_2$) would be affected, in addition, by the geometry of the roller, i.e. its size as well as the shape of the fins. Moreover, since bulk density is being estimated by the second parameter, the variety of the seed should be also considered when developing the model.

Eventually, assuming empirical linear relationship between the mass flow and the sensor output information was successful in estimating the mass flow at the experimented range of roller speeds. However, a future improvement on the estimation model, so that a wider range of granular materials at wider mass flow rates could be covered, seemed possible if one or more of the following suggestions would be followed:

a. Installing an additional fibre sensor 1 on the sensor platform to detect the clumps from two sides simultaneously. This arrangement will reduce occlusion especially in heavy clumps. The density of the clump would, therefore, be based on the output voltage of two sensors resulting in a higher accuracy in estimating wider range of clumps by the same model.

b. Reducing the period of time to 0.1 s rather than 0.8 s so that overlaps in the periods of time could be avoided. This would be achieved by using a scale of higher sampling rate.

c. Reconstructing the regression model assuming non-linearity, as the results of the linear model showed tendency to underestimate big clumps and overestimate small clumps consistently.

4. Conclusion

In order to estimate the mass of grain seeds flowing in clumps during sowing, an off-the shelf digital fibre sensor was used to detect the length and the density of the clumps of seeds. The indoor apparatus was designed so that the seeds would flow in the same rate that occurs if a grain drill runs in an average forward speed of 7 km/h. This was achieved by running the fluted roller in the apparatus at 4 rpm primarily, as well as at 2 and 6 rpm to cover the whole possible range of mass flow.

Assuming linear relationship between the sensor parameters and the mass of the clumps, the mass flow was estimated using multiple linear regression analysis. However, the minimum time interval was 0.8 s because of the limitations of the mass measuring scale. This additional assumption may have affected the 1 estimation of each clump independently as many clumps were overlapped between successive time intervals. This also caused an overestimation of light clumps, whilst caused an underestimation of heavy clumps.

Nevertheless, the methodology was successful in estimating the mass of a continuous flow of seed clumps. The average difference in estimation at 4 rpm was 0.9%, while the overall error in estimating flow rates at all speeds was 5.3%, where there was overestimation at 2 rpm and underestimation at 6rpm. These results showed that the digital fibre sensor can be used on the grain drill for estimating seed at variable sowing rates within certain speed limits. Moreover, the results showed evidence that the sensor can be used to cover a wider range of flow rates of different granular materials. This

might be achieved careful calculation of the model parameters. Also, adding one more fibre sensor to reduce the occlusion effect or considering non-linearity between the parameters in a wider range of flow rates would contribute in additional improvement of the model.

Acknowledgement

A part of this research was supported by the commissioned project of the Ministry of Agriculture, Forestry, and Fisheries entitled by "Development of automatic and assistant agricultural system for laboursaving in agriculture work (2010-2014)", Under the sub division of "Development of Land-based Autonomous Agricultural Production System on Rice, Wheat, and Soybeans".

Reference

Grift, T.E. 2001. Mass flow measurement of granular 1 materials in aerial application – Part 1: Simulation and modeling. Transactions of the ASAE, 44(1), 19–26

Grift, T. E., Crespi, C.M. 2008a. Estimating mean particle diameter in free-fall granular particle flow using a Poisson model in space. J. Biosystems Engineering. 101, 28– 35.

Grift, T. E., Crespi, CM. 2008b. Estimation of the flow rate of free falling granular particles using a Poisson model in time. J. Biosystems Engineering. 101, 36–41.

Grift, T.E., Hofstee, J.W. 1997. Measurement of velocity and diameter of individual fertilizer particles by an optical method. J . Agricultural Engineering Research . 66 , 235 – 238.

Grift, T.E., Walker, J.T., Hofstee, J.W. 2001. Mass flow measurement of granular

materials in aerial application – part 2: Experimental model validation. Transactions of the ASAE, 44(1), 27–34.

Karayel, D., Wiesehoff, M., Zmerzi A.O., Muller, J. 2006. Laboratory measurement of seed drill seed spacing and velocity of fall of seeds using high-speed camera system. Computers and Electronics in Agriculture. (50), 89–96

Kocher, M.F., Lan, Y., Chen, C., Smith, J.A., 1998. Opto-electronic sensor systems for rapid evaluation of planter seed spacing uniformity. Trans. ASAE 41 (1), 237-245.

Lan, Y., Kocher, M.F., Smith, A. 1999. Opto-1 electronic sensor system for laboratory measurement of planter seed spacing with small seeds. Journal of Agricultural Engineering Research. 72, 119–127.

Navid, H., Ebrahimian, S., Gassemzadeh, H.R., Mousavi nia, M. J. 2011. Laboratory evaluation of seed metering device using image processing method. Australian Journal of Agricultural Engineering. 2(1), 1-4.

ONAL, O., ONAL, I. 2009. Development of a computerized measurement system for in row seed spacing accuracy. Turkic Journal of Agriculture & Forestry. 33, 99-109.

R-Project .2013. The R Project for Statistical Computing. Available at http://www.r10 project.org Accessed 2013 January 21.

List of Figures

Figure 1. Sketch of the components of the digital fibre sensor (amplifier, emitter, receiver, and fibre cables). The beam of light from the emitter toward the receiver covering the area in which seeds fall

Figure 2. Indoor apparatus which resembles the mass flow of seeds in grain drill

Figure 3. Plot of mass of seeds clumps as received by digital scale during one trial of the experiment

Figure 4. Raw data as received from the digital fiber sensor and the digital scale (Left), and the procedure of arranging them in samples according to the designated period of time (right). Samples in grey are calculated using the raw data listed at the left

Figure 5. Plot of actual mass measured by the digital scale versus estimated mass using the regression model of Trial 4 when the period of time was 0.8 s (a), 1.6 s (b), and 2.4 s (c)

Figure 6. Actual mass measured manually by scale versus estimated mass using the regression model for 1903 clumps when the time interval was 0.8 s

Figure 7. Actual mass measured manually by scale versus estimated mass using the regression model of each entire trial. Solid markers represent the trials whose data were used in modelling.

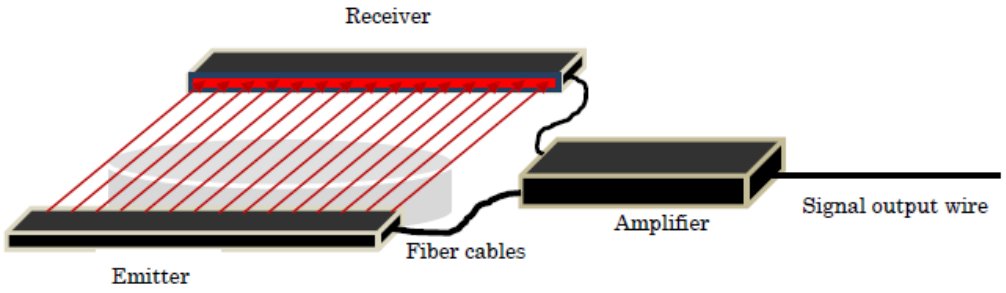

Figure 1. Sketch of the components of the digital fibre sensor (amplifier, emitter, receiver, and fibre cables). The beam of light from the emitter toward the receiver covering the area in which seeds fall

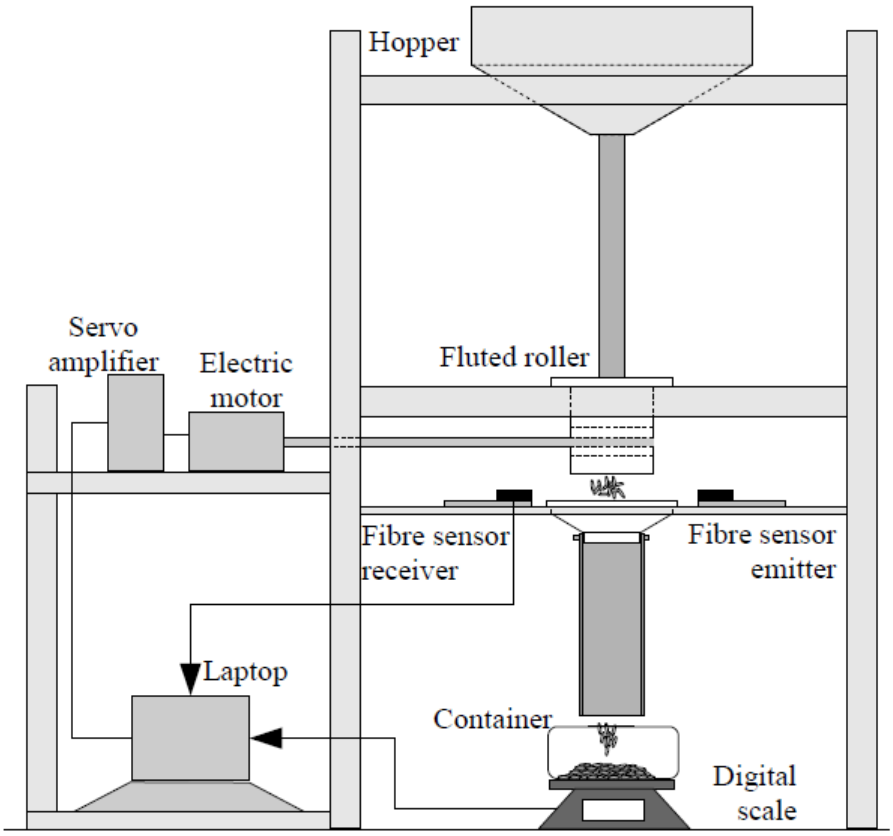

Figure 2. Indoor apparatus which resembles the mass flow of seeds in grain drill

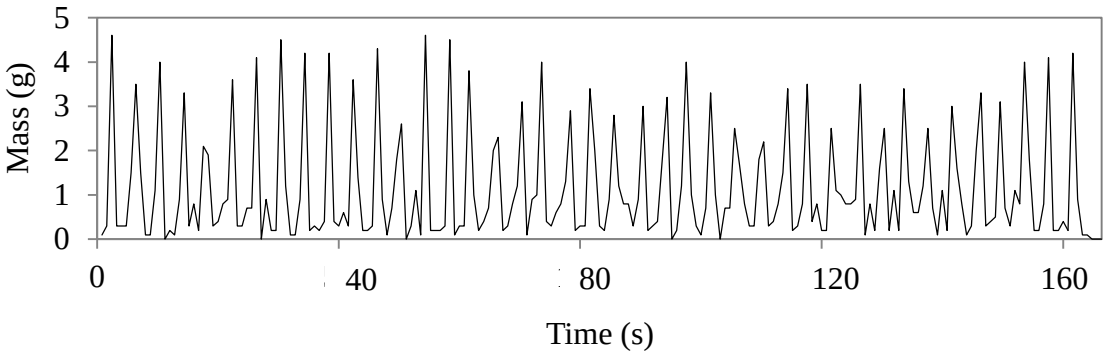

Figure 3. Plot of mass of seeds clumps as received by digital scale during one trial of the experiment

Raw data

Fibre sensor data	Scale data
Output voltage *v* (*v*)	Accumulative mass *M* (g)
4.91	53.0
4.91	
4.91	
4.91	
4.86	
4.91	
4.91	
4.91	
4.91	57.2
4.91	
4.85	
4.64	
4.46	
4.69	
4.85	
4.91	
4.59	57.6
4.91	
4.91	
4.91	
4.91	
4.91	
4.91	
4.91	57.9
4.91	
4.91	
4.91	
4.91	
4.91	
4.91	
4.81	

Samples arrangement

Mass *(m)*	Density of clump *(d)*	*Length* *(l)*
at *0.8 s*		
0.2	0.00	0
0.4	0.05	0
4.2	1.09	5
0.4	0.32	1
0.3	0.11	1
0.6	0.02	1
0.3	1.01	3
at *1.6 s*		
1	0.28	0
4.4	1.91	5
0.5	0.01	1
4.6	1.14	5
0.7	0.43	2
0.9	1.02	7
5	2.29	4
at 2.4 s		
5.9	2.073	4
1.1	0.275	1
4.7	1.912	4
4.9	1.141	7
1.3	0.442	1
5.3	3.301	11
0.7	0.003	0

Figure 4. Raw data as received from the digital fiber sensor and the digital scale (Left), and the procedure of arranging them in samples according to the designated period of time (right). Sample in grey are calculated using the raw data listed at the left.

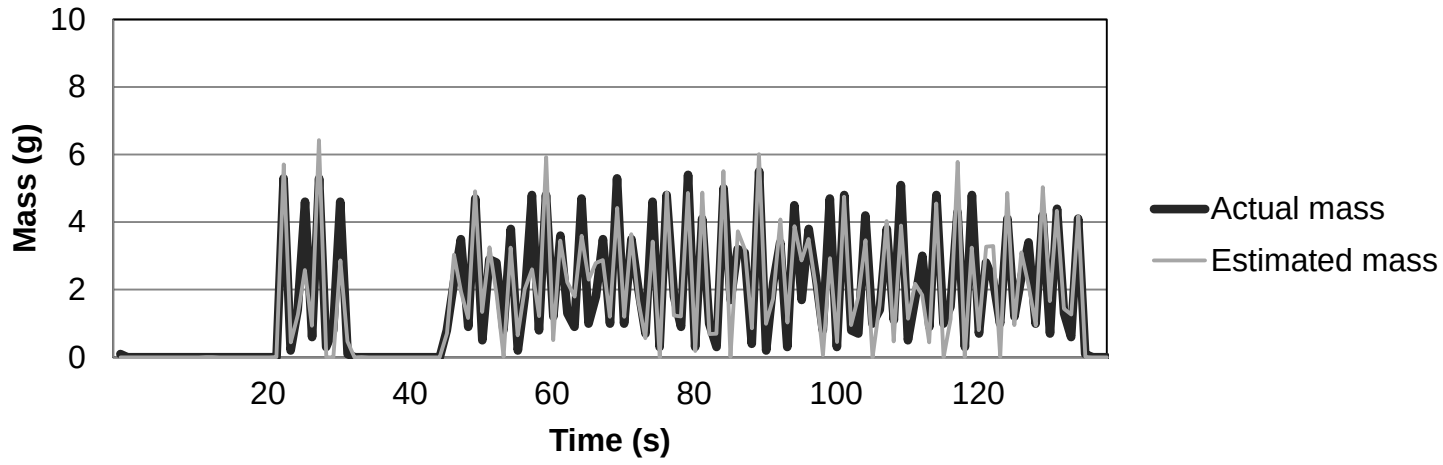

(a)

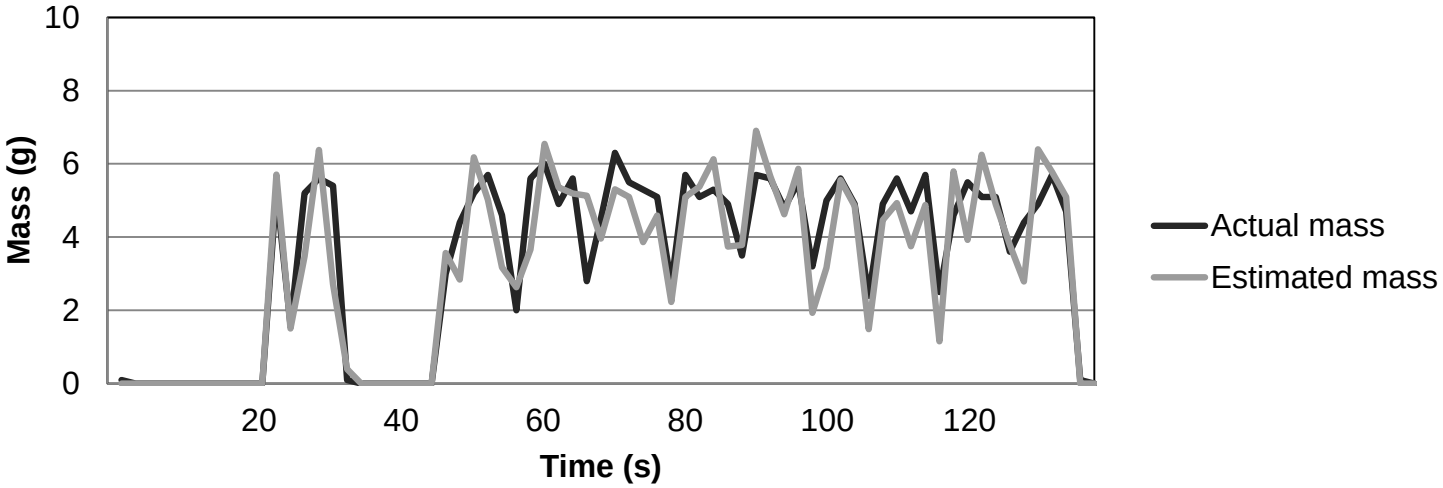

(b)

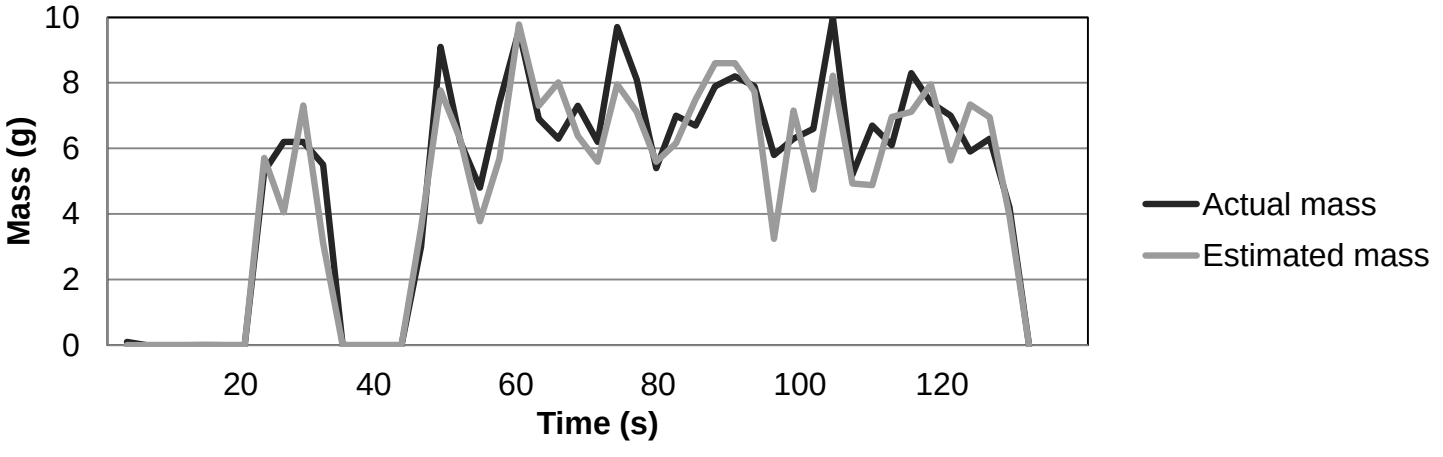

(c)

Figure 5. Plot of actual mass measured by the digital scale versus estimated mass using the regression model of Trial 4 when the period of time was 0.8 s (a), 1.6 s (b), and 2.4 s (c)

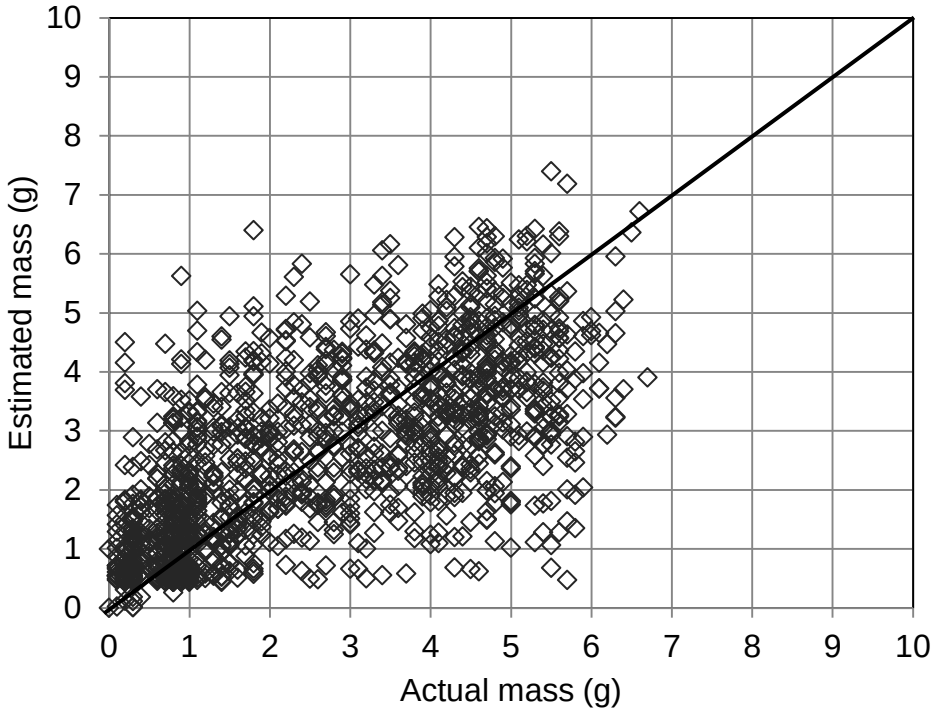

Figure 6. Actual mass measured manually by scale versus estimated mass using the regression model for 1903 clumps when the time interval was 0.8 s

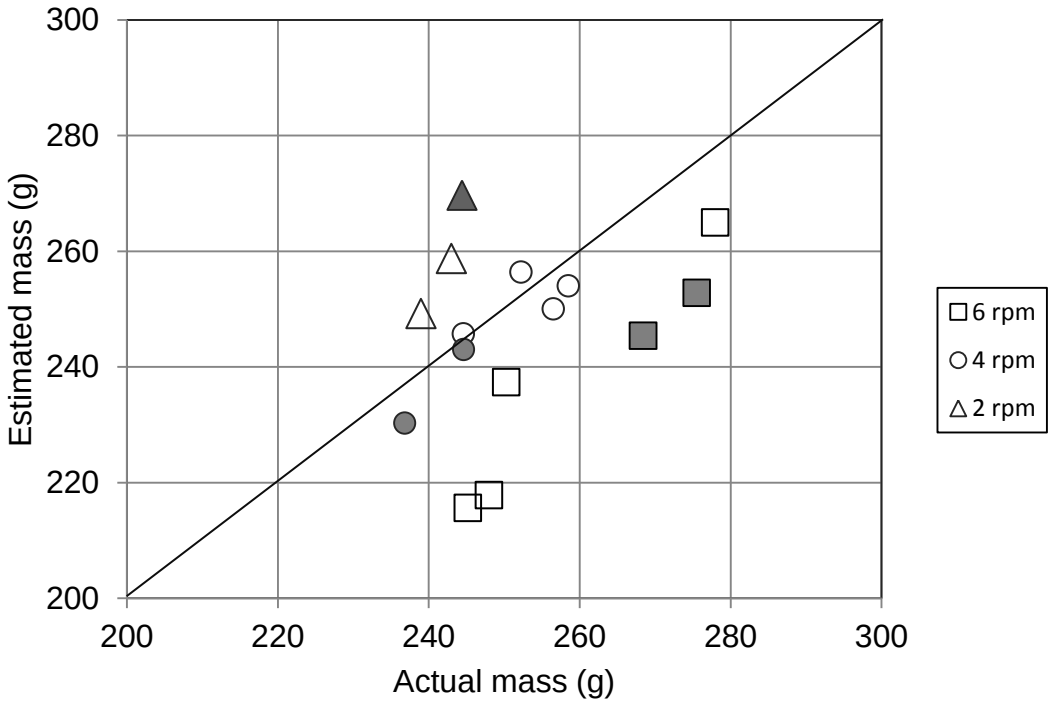

Figure 7. Actual mass measured manually by scale versus estimated mass using the regression model of each entire trial. Solid markers represent the trials whose data were used in modelling.

Table 1. Time, speed, as well as mass measured and estimated at each trial

Trial	1	2	3	4	5	6	7	8	9	10	11	12	13	14	15
Time (s)	162	166	162	110	84	88	83	86	118	63	57	64	62	50	57
Speed (rpm)	2	2	2	4	4	4	4	4	4	6	6	6	6	6	6
Actual mass (g)	244.6	239	243	236.8	252.2	244.6	244.6	256.5	258.5	275.4	250.3	278	268.4	248	245.2
Estimated mass (g)	269.7	249.2	258.7	230.3	256.4	245.7	243.0	250.0	254.0	252.8	237.3	264.9	245.4	217.8	215.6
Estimation error (%)	-10.3	-4.3	-6.5	2.7	-1.7	-0.5	0.6	2.5	1.7	8.2	5.2	4.7	8.6	12.2	12.1

Table 2. Number of samples of clumps collected at each speed using different time intervals

Speed (rpm)	*n*=1 (time = 0.8 s)	*n*=2 (time = 1.6 s)	*n*=3 (time = 2.4 s)
2	930	465	310
4	661	220	147
6	312	156	104
Total	1903	841	561

Table 3. Values of models coefficients generated assuming different periods of time

Period of time (s)	Coefficients of the models	
	β_1	β_2
0.8	1.066	0.438
1.6	0.944	0.498
2.4	1.046	0.477

Table 4. Comparison of heavy clumps as obtained at running the fluted roller at different speeds

Speed (rpm)	Heavy Clumps				
	Average number	Average mass (g)	Mass (%)	Frequency (clump/s)	Max. mass (g)
2	65.8	2.97	79	0.40	6.0
4	64.8	3.34	87	0.78	6.2
6	65.3	3.87	96	1.12	6.7